

Current-Driven Magnetic Excitations in Permalloy-Based Multilayer Nanopillars

S. Urazhdin, Norman O. Birge, W. P. Pratt Jr., and J. Bass

Department of Physics and Astronomy, Center for Fundamental Materials Research and Center for Sensor Materials, Michigan State University, East Lansing, MI 48824

We study current-driven magnetization switching in nanofabricated $\text{Ni}_{84}\text{Fe}_{16}/\text{Cu}/\text{Ni}_{84}\text{Fe}_{16}$ trilayers at 295 K and 4.2 K. The shape of the hysteretic switching diagram at low magnetic field changes with temperature. The reversible behavior at higher field involves two phenomena, a threshold current for magnetic excitations closely correlated with the switching current, and a peak in differential resistance characterized by telegraph noise, with average period that decreases exponentially with current and shifts with temperature. We interpret both static and dynamic results at 295 K and 4.2 K in terms of thermal activation over a potential barrier, with a current dependent effective magnetic temperature.

PACS numbers: 73.40.-c, 75.60.Jk, 75.70.Cn

The effects of magnetic order on transport, e.g. giant magnetoresistance, are well studied and widely used in technology. The discovery of predicted [1, 2] current-induced magnetization precession [3, 4] and switching [5] stimulated an explosion of interest in the reverse effect of the current on magnetic order and magnetic dynamics. Besides fundamental interest in the physics of magnetic systems driven far out of equilibrium, these phenomena hold promise for high-density memory applications. With the number of theoretical papers growing rapidly [6]-[15], relatively few experimental facts are known, mostly for Co/Cu/Co multilayers, and, for nanofabricated samples, mostly at room temperature, $T=295$ K [16]-[23].

By studying Py/Cu/Py (Py=Permalloy= $\text{Ni}_{84}\text{Fe}_{16}$) nanofabricated trilayers (nanopillars), we are able for the first time to quantitatively compare current-driven switching at 295 K and 4.2 K. Much smaller crystalline anisotropy and magnetoelastic coefficients of Py eliminate the irregular behavior at 4.2 K seen in Co/Cu/Co by others [19] and confirmed by us. Our data let us study temperature dependences, and establish general features of switching in both the hysteretic switching regime at low magnetic field H and the reversible switching regime at higher H . We emphasize two important findings. (1) In a new picture of the physics in the reversible regime, we isolate two different phenomena: (a) magnetic excitations occurring above a threshold current I_t , and appearing either as a linear rise or peaks in differential resistance, dV/dI ; and (b) the more well known reversible switching peak. We show that the latter arises from telegraph noise switching of magnetization between parallel (P) and antiparallel (AP) orientations, and occurs when the dwell times in the P and AP states are approximately equal, $\tau_P \approx \tau_{AP}$. (2) Extending an idea of Ref. [21], we describe incoherent magnetic excitation by current in both hysteretic and nonhysteretic switching regimes in terms of an effective magnetic temperature T_m , which can differ substantially from the lattice temperature T_{ph} . Our model leads to a temperature depen-

dence of the switching that differs from expectation for models [15, 19] based on coherent current-driven excitation of the uniform precession [1].

Our samples were nanofabricated with a multistep process similar to that used by others [5]. To minimize dipolar coupling between the Py layers, we used the geometry of Albert *et al.* [16], with the bottom (thicker) Py layer left extended, and the top Py layer and Cu spacer patterned into an elongated shape with typical dimensions 130×60 nm. The bottom Py and the Cu spacer thicknesses were always 20 nm and 10 nm, respectively (we give all thicknesses in nm). The patterned Py layer thickness was varied from 2 to 6 nm. We measured differential resistances, dV/dI , with four-probes and lock-in detection, adding an ac current of amplitude $20 \mu\text{A}$ at 8 kHz to the dc current I . Most of 12 Py/Cu/Py devices studied had resistances $R \approx 1.5 \Omega$, magnetoresistance (MR) $\approx 5\%$ at 295 K, and $\text{MR} \approx 8\%$ at 4.2 K. Positive current flows from the extended to the patterned Py layer. H is directed along the easy axis of the nanopillar.

Figs. 1(a,b) show the variations of dV/dI with I for a patterned Py(20)/Cu(10)/Py(6) trilayer at 295 K (1a) and 4.2 K (1b), for $H = 50$ Oe (solid curves) and $H = 500$ Oe (dashed curves). The insets show the variations with H for $I = 0$. At small H , the magnetization switches hysteretically to a higher resistance AP state at a large enough positive current $I_s^{P \rightarrow AP} \equiv I_s$, and to a low resistance P state at negative $I_s^{AP \rightarrow P}$. At larger H , the switching step turns into a nonhysteretic peak. Figs. 1(c,d) show the switching diagrams at 295 K and 4.2 K, extracted from data such as those in Figs. 1(a),(b), obtained both by varying I at fixed H and H at fixed I . Qualitatively, the 295 K data in Figs. 1(a,c) are similar to those published previously for Co/Cu/Co [16]. As expected, both the reduced magnetization and thermal activation result in smaller switching currents and fields $H_s(I = 0)$ at 295 K. The slight H -asymmetry in Figs. 1(c,d) is attributed to a combination of the current-induced Oersted field and sample shape asymmetry.

The first important new feature of our data is the

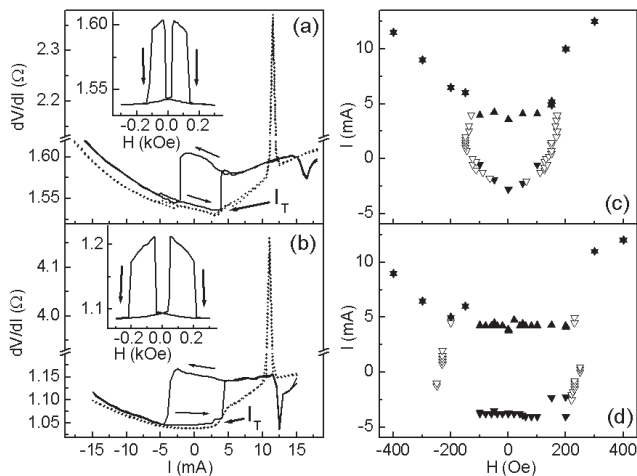


FIG. 1: (a) Switching with current at 295 K in a Py(20)/Cu(10)/Py(6) trilayer (thicknesses are in nm). Solid line: $H = 50$ Oe, dashed line: $H = -500$ Oe. Arrows mark the scan direction. I_t is the threshold current as defined in the text. Inset: MR dependence on H at $I = 0$. (b) Same as (a), at 4.2 K. (c),(d) Magnetization switching diagram, extracted from the current-switching at fixed H (solid symbols), and field-switching at fixed I (open symbols): (c) at 295 K, (d) at 4.2 K. Downward triangles: AP to P switching, upward: P to AP switching. The reversible switching peaks are marked by coinciding upward and downward triangles.

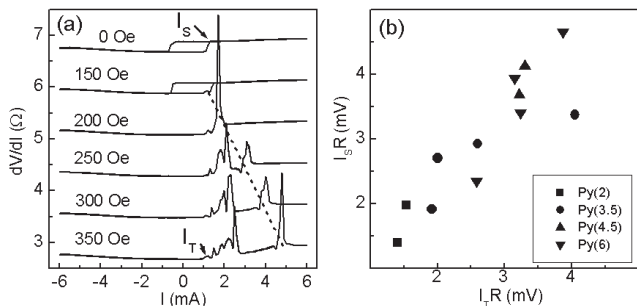


FIG. 2: (a) Differential resistance of a Py(20)/Cu(10)/Py(3.5) trilayer for various H , at 4.2 K. $R_P = 3.6$ Ω, $R_{AP} = 4.0$ Ω, curves are offset for clarity. Dashed line follows the reversible switching peak. The onset of the peaks in R_P is marked by I_t , and I_s is the $P \rightarrow AP$ switching current at $H = 0$. (b) Relation between the $P \rightarrow AP$ switching current I_s at $H = 0$, $T = 4.2$ K and the threshold current I_t (as defined in the text) for 12 samples with patterned Py layer thicknesses: 2 nm (squares), 3.5 nm (diamonds), 4.5 nm (triangles), 6 nm (circles). I_s , I_t are multiplied by the resistances R of the samples.

almost square shape of the hysteretic region at 4.2 K (Fig. 1(d)). At 4.2 K, the switching currents do not change in the range -230 Oe $< H < 230$ Oe, beyond which the switching becomes reversible. Similarly, for -4 mA $< I < 4$ mA, $H_s(I)$ is independent of I , and at larger positive I the switching becomes reversible.

The second important new feature is a threshold cur-

rent I_t (labeled in Figs. 1(a,b) and Fig. 2(a)) seen at large H , with reversible switching. Most of our Py/Cu/Py and Co/Cu/Co samples showed a nearly linear rise of $(dV/dI)_P \equiv R_P$ above I_t . Similar behavior was likely present in earlier Co/Cu/Co data at 295 K, but less obvious, and thus rarely noted [25]. In our smallest sample, (Fig. 2(a), dimensions estimated at 50×100 nm), the linear rise is resolved at 4.2 K into several peaks. They appear only to the left of the reversible switching peak, as the latter moves to higher I with increasing H (shown by a dashed line). We observed similar, less pronounced peak structures in some samples with smaller R . Remarkably, in all cases (e.g. Figs. 1(a,b), Fig. 2(a)), the onset of a linear rise or peak structures in R_P coincides with $I_s(H = 0)$. Within the uncertainty in determining the onset current I_t , we find $I_s = I_t$ for all 12 samples studied (Fig. 2(b)). This correlation between I_s and I_t , combined with the abruptness of the changes with I in Fig. 1(d), point to the importance of I_t . Moreover, upon following the data up to $H = 4$ kOe (not shown), we find I_t to be almost independent of H (increasing by only 10–40% for different samples).

We identify I_t as a threshold for magnetic excitation of the patterned Py layer. An excitation threshold was previously seen as a peak in the differential resistance of point-contacts on extended magnetic multilayers [3, 4]. In nanopillars, this threshold behavior is modified into a linear rise or peak structures. The reversible switching peak appears at higher H , and evolves faster with H (dashed line in Fig. 2(a)) than the peaks we attribute to magnetic excitations. Time-resolved measurements of resistance, at I and H close to the reversible switching peak (Fig. 3(a)), show that the reversible switching is characterized by telegraph noise with random distribution of τ_P , τ_{AP} . Similar slow telegraph noise was reported in a point contact at one current [3], and at the transition point from hysteretic to reversible switching in Co/Cu nanopillars at 295 K, at I or H fixed [19].

The data of Fig. 3(b,c), and the finding that the reversible switching peak is a consequence of telegraph noise and occurs at $\tau_P \approx \tau_{AP}$, represent our third new experimental result. Fig. 3(b) shows that, when both I and H are increased so as to hold $\tau_P = \tau_{AP}$, the average period of the telegraph noise decreases exponentially with similar slopes at 295 K and 4.2 K, down to the 1 MHz bandwidth limit of our setup. Fig. 3(c) shows that the variations of τ_P , τ_{AP} with I have similar forms at 295 K and 4.2 K. These data (as well as similar data for Co/Cu at 295 K [19, 24]) show that the reversible switching peak does not indicate abrupt onset of a new physical process. At small I , $\tau_P \gg \tau_{AP}$, and the average sample resistance is close to R_P , while at large I , $\tau_P \ll \tau_{AP}$, and the average resistance is close to R_{AP} . The reversible switching peak appears in dV/dI at $\tau_P \approx \tau_{AP}$, due to the exponential variation of τ_P , τ_{AP} with I . Thus, it merely reflects the current-dependent

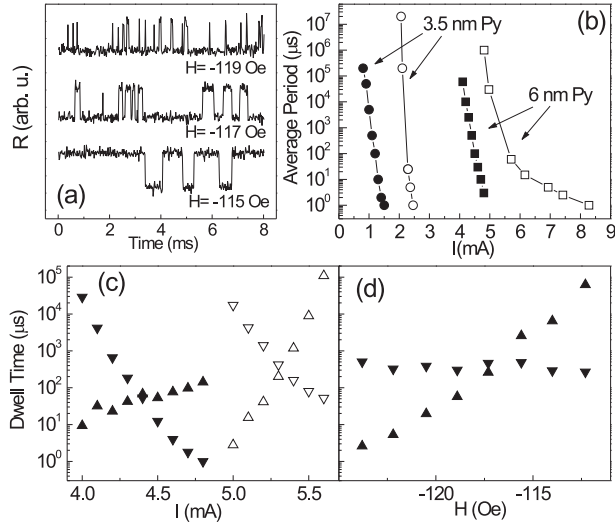


FIG. 3: (a) Time traces of the Py(20)/Cu(10)/Py(6) sample static resistance $R = V/I$ at $I = 4.4$ mA, $T = 295$ K at different H . (b) Current dependence of the average telegraph noise period for Py(20)/Cu(10)/Py(6) (squares) and Py(20)/Cu(10)/Py(3.5) (circles) samples. Open symbols: $T = 4.2$ K, filled symbols: $T = 295$ K. H was adjusted so that the average dwell times in AP and P states were equal. (c) The dependence of the P (downward triangles) and AP (upward triangles) dwell times on I , for a Py(20)/Cu(10)/Py(6) sample. Open symbols: $T = 4.2$ K, $H = -335$ Oe, filled symbols: $T = 295$ K, $H = -120$ Oe. (d) Dependence of P (downward triangles) and AP (upward triangles) dwell times on H at $I = 4.4$ mA, $T = 295$ K.

telegraph noise statistics; I_t is the only fundamental current related to magnetic excitations. The amplitude and inverse width of the reversible switching peak are proportional to $d[(\tau_{AP} - \tau_P)/(\tau_{AP} + \tau_P)]/dI$. In Fig. 2(a), they are correlated with the positions of the peaks that we attribute to magnetic excitations. For example, at 200 Oe, the reversible peak is on top of the magnetic excitation peaks, and is significantly taller and narrower than at higher H . More detailed data and analysis will be presented elsewhere [26].

We interpret both our static and dynamic results consistently in terms of a model involving thermally activated switching over a one-dimensional potential barrier, with an effective current-dependent temperature $T_m(I)$ [21], and a threshold current, I_t . T_m can differ from the lattice temperature T_{ph} in confined geometry, where the magnetic energy relaxes significantly more slowly than the highly excited individual magnetic modes [27]. Formally, a potential energy barrier is inconsistent with the current-driven torque in the Landau-Lifshitz-Gilbert equation [1]. Li and Zhang [15] have shown that the work performed by the torque leads to

a current-dependent effective switching barrier, but with $T_m = T_{ph}$, which we shall see is inconsistent with our data of Fig. 3(b,c).

Our observation that I_t varies only weakly with H up to 4 kOe provides information about whether its origin is quantum mechanical [2] or classical [1]. In the quantum model, I_t follows from $\Delta\mu = \hbar\omega$, where $\Delta\mu$ is the current dependent difference in chemical potentials of spin-up and spin-down electrons due to spin accumulation, and ω is the magnon frequency. At small H , $I_t \propto \omega \propto \sqrt{1 + H/H_a}$ [28], where H_a is the in-plane anisotropy field. In our samples, $H_a \approx 300$ Oe, giving much too rapid an increase of I_t with H . In the classical treatment based on the Landau-Lifshitz-Gilbert equation, I_t is set by the balance between the torque induced by the spin polarized current and Gilbert damping. The H dependence of I_t is much weaker $I_t(H) \approx I_t(0)[1 + H/(2\pi M)]$ [5], where M is the magnetization, $M \approx 880$ Oe for Py. This model predicts $\frac{dI_t(H)}{I_t(0)dH} \approx 0.2$ (kOe) $^{-1}$, not too far from the measured values of 0.03–0.1 for different samples.

To analyze our data quantitatively, we determine the dwell times $\tau_{P,AP}$ by

$$\tau_{P,AP} = \frac{1}{\Omega} \exp \left[\frac{U_{P,AP}}{kT_m^{P,AP}} \right], \quad (1)$$

and approximate T_m by the heuristic relation

$$T_m = T_{ph} + K(I - I_t) \text{ for } I > I_t. \quad (2)$$

Here K is a constant, $\Omega \approx 10^7 \text{s}^{-1}$ [29] is the effective attempt frequency, $U_{P,AP}$ is the potential barrier height for switching from the P or AP state, and $T_m^{AP}(I) \neq T_m^P(I)$ when $I \neq 0$. The switching barriers $U_{P,AP}$ depend on I only through the variation of the magnetization with temperature T_m . In the P state, at $I > I_t$, magnetic excitation leads to increase of T_m^P , as illustrated in Fig. 4(a). A thermally activated transition into the AP state occurs at $kT_m^P \approx \frac{U_P}{\ln(t_{exp}\Omega)} \approx \frac{U_P}{16}$, based on the data acquisition time t_{exp} of 1 second per point. The conditions for magnetic excitation are not satisfied in the AP state, so the magnetic system cools to $T_m^{AP} \approx T_{ph}$ and at $H < H_s$ becomes trapped in this state. At $H > H_s$ (Fig. 4(b)), $kT_{ph} > \frac{U_{AP}}{16}$, i.e. the $AP \rightarrow P$ transition is also thermally activated, leading to telegraph noise at $I > I_s$, $H > H_s$.

The 4.2 K switching diagram of Fig. 1(d) is consistent with this model. It reflects the weak variations of I_t with H , and of T_m (and thus H_s) with I below I_t . We attribute the rounding of the 295 K diagram at $I < 0$ to enhancement of thermal fluctuations of magnetization by current, not included in the heuristic Eq. (2). Increasing H decreases U_{AP} , so that even these weak excitations can activate the $AP \rightarrow P$ transition. This process is described in different terms in Ref. [15].

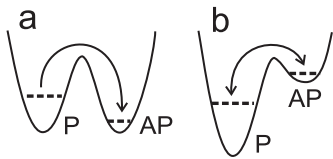


FIG. 4: (a) Schematic of current-driven hysteretic magnetization switching at $H = 0$. Dashed lines indicate T_m . (b) Schematic of telegraph noise at $H > H_s$.

The dependencies of nonhysteretic switching on I , H , and T shown in Fig. 3(b-d) agree with Eqs. (1) and (2). As I increases with H fixed, τ_P decreases exponentially because of the increase of T_m^P with $I > I_t$. An increase of τ_{AP} with I may be evidence for cooling of the magnetic system of the patterned layer in the AP state at $I > 0$, through a magnon absorption mechanism inverse to the magnon emission in the P state. At $T_{ph}=4.2$ K, the requirement for telegraph noise ($U_{AP} < 16kT_{ph}$) is satisfied with much smaller U_{AP} than at 295 K. Hence a slight decrease in T_m^{AP} with I has a stronger effect on τ_{AP} at 4.2 K than at 295 K, as seen in Fig. 3(c). The dependencies in Fig. 3(d) follow from $\frac{\partial \ln \tau_{P,AP}}{\partial H} = \frac{1}{kT_m^{P,AP}} \frac{\partial U_{P,AP}}{\partial H}$. Since $T_m^P > T_m^{AP}$, τ_P varies with H more slowly than τ_{AP} . Based on the data of Fig. 3, we estimate the dependence $T_m(I)$ numerically. Some of our Py(20)/Cu(10)/Py(3.5) and all of the Py(20)/Cu(10)/Py(2) samples were superparamagnetic at 295 K. Assuming linear variation of the switching barrier with nanopillar thickness, we estimate the switching barrier $U_{P,AP}(H = 0) \approx 0.7$ eV for Py(20)/Cu(10)/Py(6) samples. We use an approximate dependence $U(T_m) = U_0 \sqrt{1 - T_m/T_c}$, where $T_c = 800$ K is the Curie temperature for Py. Using $d \ln(\tau_P)/dI = 11$ (mA) $^{-1}$ from Fig. 3(c), we obtain from Eq. (1) $K = \frac{dT_m^P}{dI} \approx 400$ K/mA. Both the 295 K (filled symbols in Fig. 3(c)) and 4.2 K data (open symbols) are approximately consistent with this estimate. In contrast, starting from a current-dependent effective barrier with $T_m = T_{ph}$ [15, 19], one would predict $\frac{d \ln(\tau_P(I))}{dI} \approx \frac{U_P}{I_c k T_{ph}}$, where I_c is the switching current at $T = 0$. This strong dependence on T_{ph} disagrees with the similarity of the 4.2 K and 295 K data.

To summarize, our major new experimental results on Py/Cu/Py nanopillars are: i) a square switching diagram at 4.2 K; ii) an onset current I_t (closely related to the hysteretic switching current I_s) for a linear rise of dV/dI in larger samples or a series of peaks in smaller ones; iii) reversible switching, characterized by telegraph noise with rate both increasing exponentially with I and shifting with temperature. The reversible switching peak in dV/dI occurs when the dwell times in the P and AP states are approximately equal. We are able to explain

the hysteretic switching behavior at both 295 K and 4.2K, and variations of telegraph noise with I , H , and T , by means of a threshold current for the onset of magnetic excitations and thermally activated switching with a current-dependent magnetic temperature.

We acknowledge helpful communications with R. Loloee, H. Kurt, M.I. Dykman, M.D. Stiles, A.H. MacDonald, D.C. Ralph, S. Zhang, A. Fert, support from the MSU CFMR, CSM, the MSU Keck Microfabrication facility, the NSF through Grants DMR 02-02476, 98-09688, and 00-98803, and Seagate Technology.

-
- [1] J. Slonczewski, *J. Magn. Magn. Mater.* **159**, L1 (1996).
 - [2] L. Berger, *Phys. Rev.* **B 54**, 9353 (1996).
 - [3] M. Tsoi *et al.*, *Phys. Rev. Lett.* **80**, 4281 (1998); **81**, 493(E) (1998).
 - [4] M. Tsoi *t al.*, *Nature (London)* **406**, 46 (2000).
 - [5] J. A. Katine *et al.*, *Phys. Rev. Lett.* **84**, 3149 (2000).
 - [6] J. Slonczewski, *J. Magn. Magn. Mater.* **195**, L261 (1999).
 - [7] L. Berger, *Phys. Rev.* **B 59**, 11465 (1999).
 - [8] X. Waintal *et al.*, *Phys. Rev.* **B 62**, 12317 (2000).
 - [9] J. Z. Sun, *Phys. Rev.* **B 62**, 570 (2000).
 - [10] A. Brataas, Yu. V. Nazarov, and Gerrit E. W. Bauer, *Phys. Rev. Lett.* **84**, 2481 (2000).
 - [11] C. Heide, P. E. Zilberman, and R. J. Elliott, *Phys. Rev.* **B 63**, 064424 (2001).
 - [12] Ya. B. Bazaliy, B. A. Jones, and S. C. Zhang, *J. Appl. Phys.* **89**, 6793 (2001).
 - [13] S. Zhang, P. M. Levy, A. Fert, *Phys. Rev. Lett.* **88**, 236601-1 (2002).
 - [14] M. D. Stiles and A. Zangwill, *Phys. Rev.* **B 66**, 014407-1 (2002).
 - [15] Z. Li and S. Zhang, cond-mat/0302339.
 - [16] F. J. Albert *et al.*, *Appl. Phys. Lett.* **77**, 3809 (2000).
 - [17] J. Grollier *et al.*, *Appl. Phys. Lett.* **78**, 3663 (2001).
 - [18] J. Grollier *et al.*, *Phys. Rev.* **B 67**, 174402 (2003).
 - [19] E. B. Myers *et al.*, *Phys. Rev. Lett.* **89**, 196801 (2002).
 - [20] F. J. Albert *et al.*, *Phys. Rev. Lett.* **89**, 226802 (2002).
 - [21] J. E. Wegrowe *et al.*, *J. Appl. Phys.* **91**, 6806 (2002).
 - [22] J. Z. Sun *et al.*, *J. Appl. Phys.* (in press).
 - [23] B. Oezylmaz *et al.*, cond-matt/0301324.
 - [24] S. Urazhdin *et al.*, cond-mat/0303614.
 - [25] In Ref. [18], a rise of the P state resistance was noted, but described as a progressive reversal to the AP state, that would not display the widely seen reversible switching peak in dV/dI .
 - [26] S. Urazhdin *et al.*, to be published.
 - [27] J. Miltat, G. Albuquerque, and A. Thiaville in *Spin Dynamics in Confined Magnetic Structures I*, Springer, New York, 2002.
 - [28] The field dependence of the uniform magnon frequency is given in Eq.(41) Ch.(16) of C. Kittel, *Introduction to Solid State Physics*, 7th edition, John Wiley & Sons, NY, 1996.
 - [29] R. H. Koch *et al.*, *Phys. Rev. Lett.* **84**, 5419 (2000).